Published May 1, 1988

Dynamic Relationship between the Slow Potential and Spikes in Cockroach Ocellar Neurons

MAKOTO MIZUNAMI and HIDEKI TATEDA

From the Department of Biology, Kyushu University, Fukuoka 812, Japan

ABSTRACT The relationship between the slow potential and spikes of second-order ocellar neurons of the cockroach, *Periplaneta americana*, was studied. The stimulus was a sinusoidally modulated light with various mean illuminances. A solitary spike was generated at the depolarizing phase of the modulation response. Analysis of the relationship between the amplitude/frequency of voltage modulation and the rate of spike generation showed that (*a*) the spike initiation process was bandpass at ~0.5–5 Hz, (*b*) the process contained a dynamic linearity and a static nonlinearity, and (*c*) the spike threshold at optimal frequencies (0.5–5 Hz) remained unchanged over a mean illuminance range of 3.6 log units, whereas (*d*) the spike threshold at frequencies of <0.5 Hz was lower at a dimmer mean illuminance. The voltage noise in the response was larger and the mean membrane potential level was more positive at a dimmer mean illuminance. Steady or noise current injection during sinusoidal light stimulation showed that (*a*) the decrease in the spike threshold at a dimmer mean illuminance was due to the increase in the noise variance: the noise had facilitatory effects on the spike initiation; and (*b*) the change in the mean potential level had little effect on the spike threshold. We conclude that fundamental signal modifications occur during the spike initiation in the cockroach ocellar neuron, a finding that differs from the spike initiation process in other visual systems, including *Limulus* eye and vertebrate retina, in which it is presumed that little signal modification occurs at the analog-to-digital conversion process.

INTRODUCTION

In the visual system of animals, photic inputs are initially converted into slow (graded) potential signals and the graded signals are then converted into spike signals. Because the photic input that animals experience in the natural environment is a fluctuation of light intensity around a mean illuminance, the slow potential response and the spike response of visual neurons to light fluctuation have been studied (Fuortes and Hodgkin, 1964; Victor and Shapley, 1979; Tranchina et al., 1983; Chappell et al., 1985; Victor, 1987). However, little attention has been given to the dynamics of the cellular processes that convert the slow potential into spikes. A notable exception is the sine wave analysis of *Limulus* eccentric cells. Knight et al. (1970) found that the

Address reprint requests to Dr. Makoto Mizunami, Dept. of Biology, Faculty of Science, Kyushu University, Fukuoka 812, Japan.

J. GEN. PHYSIOL. © The Rockefeller University Press · 0022-1295/88/05/0703/21 $2.00
Volume 91 May 1988 703–723

magnitude of slow response is linearly converted into a spike rate in eccentric cells. Knight (1972*a*, *b*) developed an "integrate-and-fire" model for the spike initiation process, which explained well the actual spike activity of *Limulus* eccentric cells. Recently, Sakuranaga et al. (1987) found that the model can be applied to the spike discharge of catfish retinal ganglion cells. These studies suggested that the spike initiation process produces a replica of the slow potential without any major modification of the signal.

The insect ocellus is a simple photoreceptor system advantageous for studying basic mechanisms of visual signal processing. The insect ocellus contains over 100 photoreceptors and these converge onto fewer than 12 large second-order neurons, called L-neurons (Ruck, 1961; Dowling and Chappell, 1972; Goodman, 1981). Intracellular recordings from insect ocellus were first made by Chappell and Dowling (1972), who showed that a light stimulus depolarized the ocellar receptors and hyperpolarized the L-neuron of dragonfly ocelli. Incremental responses of the L-neuron have been studied in dragonflies (Chappell and Dowling, 1972) and in cockroaches (Mizunami et al., 1986). It was concluded that the incremental sensitivity of the insect L-neuron is an exact Weber-Fechner function. In addition to the graded hyperpolarizing response, the L-neuron of the cockroach exhibits spikes at the decremental phase of step stimuli or sinusoidal stimuli (Mizunami et al., 1982, 1986), as in the case of the locust L-neuron (Wilson, 1978*a*).

In the present study, we analyzed the dynamic relationship between the slow potential and spikes in the cockroach ocellar L-neuron, using sinusoidally modulated light stimuli around various mean illuminances. The cockroach L-neuron is suited for such an analysis because (*a*) stable intracellular recordings of >60 min are feasible and (*b*) a sinusoidal light modulation produces almost sinusoidal voltage modulation, thereby allowing for a high quality of sine wave analysis of the spike initiation process. Our major findings are that (*a*) the spike initiation process has bandpass filtering characteristics; (*b*) the spike initiation process contains a dynamic linearity and a static nonlinearity; (*c*) the noise in the response lowers the spike threshold: it has facilitatory effects on the spike initiation; (*d*) the noise effects are prominent when there is a low-frequency potential modulation under a dim mean illuminance; and (*e*) the mean potential level, which changes depending on the mean illuminance, has little effect on the spike threshold. We conclude that (*a*) the spike initiation process in cockroach L-neurons can be modeled by an integrate-and-fire generator, and (*b*) the spike initiation process in the L-neuron is an important step in signal processing in the cockroach ocellar system.

MATERIALS AND METHODS

Preparation

Adult males of the cockroach, *Periplaneta americana,* reared in our laboratory at Kyushu University, were studied. The whole animal was mounted dorsal side up on a Lucite stage and fixed with beeswax. The compound eyes and one of two ocelli were shielded from light by beeswax mixed with carbon black. The dorsal part of the head capsule was removed and the dorsal surface of the brain was exposed. Saline containing 1% Actinase (type E, Kaken Seiyaku, Tokyo, Japan) was applied to the brain to facilitate insertion of the electrode. The saline solution was that described by Yamasaki and Narahashi (1959).

Stimulus and Recording

Intracellular recordings from L-neurons were made using glass microelectrodes filled with 2 M potassium acetate and having a DC resistance of ~50–80 MΩ. These electrodes were inserted into L-neurons at the ocellar tract of the brain, an area at which the spikes of L-neurons initiate (Mizunami et al., 1987). Stable recordings of >60 min were feasible. These neurons were identified as L-neurons from their responses, in particular: (*a*) a hyperpolarizing response of >30 mV to a bright light stimulus, and (*b*) a large voltage fluctuation during dim light stimulation. In some preparations, the neurons were stained by injecting cobalt ions through the recording electrode and identified anatomically (see Mizunami et al., 1982). The electrodes were connected to a high-impedance, negative-capacity compensated preamplifier (MEZ-8201, Nihon Kohden, Tokyo), which was equipped so that a constant current could be passed

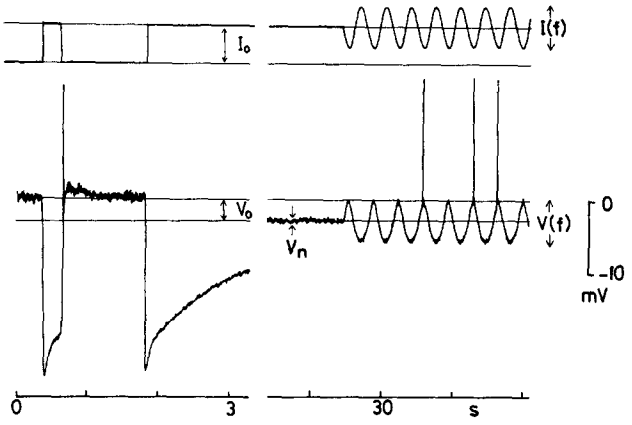

FIGURE 1. Responses of a cockroach ocellar L-neuron evoked either by a step light stimulus given in the dark or by a sinusoidally modulated light stimulus. The L-neuron responded to the sinusoidal stimulus with a sinusoidal voltage modulation, $V(f)$, around a mean voltage, V_o. A spontaneous voltage fluctuation (voltage noise), V_n, was superimposed on the modulation response. Spikes were seen at the offset of step stimulation and at the peak of the voltage modulation. The mean illuminance of the stimulus, I_o, was 20 $\mu W \cdot cm^{-2}$; the modulation frequency, f, was 2 Hz; the depth of modulation of the stimulus, $I(f)$, was 60%.

through an active bridge circuit. The magnitude of the stimulus current depended linearly on the driving voltage applied to the current-passing circuit. A small piece of platinum in the bathing solution served as an indifferent electrode.

Current-voltage relationships of L-neurons were measured using double-barreled electrodes; one barrel was used to inject the current and the other was used to record the voltage. The electrodes had a small coupling resistance of <0.4 MΩ; therefore, the current-voltage plot was obtained by subtracting the voltage drop due to electrical coupling from the recorded voltage change.

A light-emitting diode (LED; Sharp Corp., Tokyo) was used as a light source. The LED had a spectral peak at 560 nm. The LED was driven by a sinusoidal current provided by a function oscillator (ET1101, NF Design Block, Tokyo). The illuminance of the stimulus depended linearly on the magnitude of the driving current. The stimulus light was monitored by a photodiode (TFA1001W, Siemens-Allis, Inc., Cherry Hill, NJ) before being attenuated by filters. The light stimulus and cellular response were observed on an oscilloscope and stored on analog tape. Some analyses were made using a VAX 11/780 computer (Digital Equipment

Corp., Maynard, MA) with an AP120B array processor (Floating Point Systems, Portland, OR). All experiments were done at a room temperature of 20–24°C.

Analytical

The sinusoidal light stimulus consisted of two components, a steady mean, I_o, and a dynamic component, $I(f)$, as shown in Fig. 1. $I(f)$ was defined by the modulation frequency (Hertz) and the depth of modulation. The depth (percentage) is defined in the conventional fashion: $(I_{max} - I_{min})/(I_{max} + I_{min}) \times 100$, where I_{max} is the maximum illuminance and I_{min} is the minimum illuminance. The depth of modulation represents the "contrast" between the stimulus and the adapting light. The mean illuminance, I_o, was represented by $\log_{10}$ attenuation (0 log is 20 $\mu W \cdot cm^{-2}$ throughout this study). In the actual experiments, neutral density (ND) filters were interposed between the light source and the preparation to attenuate I_o. The depth of modulation of the stimulus remained unchanged by interposing ND filters.

The resulting response recorded intracellularly from cockroach ocellar L-neurons consisted of a sinusoidal slow potential modulation and spikes. The slow potential response contained three components, a steady mean potential, V_o, a voltage noise, V_n, and a modulation response, $V(f)$. V_o and V_n were related to the mean illuminance, I_o, and $V(f)$ was related to light modulation, $I(f)$. $V(f)$ was defined as $V_{peak} - V_{bottom}$, where V_{peak} is the potential at the peak and V_{bottom} is the potential at the bottom of the voltage modulation.

The magnitude of spike response could be defined as a probability of spike generation for one voltage cycle, $S(f)$, as will be discussed in the Results. The L-neuron had no maintained discharge under steady illumination or in the dark: the spike response had no steady component. We analyzed the manner in which the spike response, $S(f)$, is related to parameters of the slow potential response, $V(f)$, V_n, and V_o. We also describe briefly how each component of the slow potential response and the spike response relates to each parameter of the light stimulus. Some aspects of the relationship between the light stimulus and the slow potential response have been reported (Mizunami et al., 1986).

RESULTS

Responses to Sinusoidal Light Stimulus

The cockroach ocellus contains ~10,000 photoreceptors, which converge on four large second-order neurons, the L-neurons (Weber and Renner, 1976; Toh and Sagara, 1984). The axon of the L-neuron exits the ocellus and projects into the ocellar tract of the brain through the ocellar nerve (Mizunami et al., 1982). In the ocellar tract, L-neurons make output synapses onto several types of third-order neurons (Toh and Hara, 1984; Mizunami and Tateda, 1986).

Fig. 2 shows typical records of responses from an ocellar L-neuron to sinusoidal light modulation. Responses to stimuli with various modulation frequencies (*A*) and various modulation depths (*B*) are shown. The stimuli had a mean illuminance of 0.2 $\mu W \cdot cm^{-2}$ (−2 log units). The response of the L-neuron consisted of two components, a graded voltage fluctuation and the spikes. We refer to the former as the slow potential response and to the latter as the spike response. The waveform of the slow potential response to sinusoidal light was roughly sinusoidal, which suggests a quasilinear response. A small nonlinearity was detected in the slow potential response: the peaks of the sine wave were sharper than the trough. The nonlinearity reflects a compression of the response amplitude to an incremental (hyperpolarizing) light stimulation (Mizunami et al., 1986). The nonlinearity may also reflect a subthreshold active (regenerative) response. A solitary spike was evoked at the peak

or depolarizing phase of the modulation response. One modulation cycle of stimulus usually evoked only one spike, even when a stimulus with a large modulation depth (75%) was applied. When the modulation frequency was low (less than ~0.5 Hz) and the mean illuminance was low (less than about −3 log units), two to four spikes were frequently seen within a cycle of voltage modulation, as will be discussed later (see Fig. 6). We defined the magnitude of spike response as the rate of spike generation for one cycle of modulation stimulus. The rate of spike generation was measured as follows. The responses to 30–80 cycles of stimulus were recorded, and the rate of spikes was calculated by dividing the number of voltage modulation cycles in which spikes were generated by the total number of the cycles. Both the peak-to-peak amplitude of the slow response and the rate of spikes depended on the modulation frequency and the modulation depth of the stimulus.

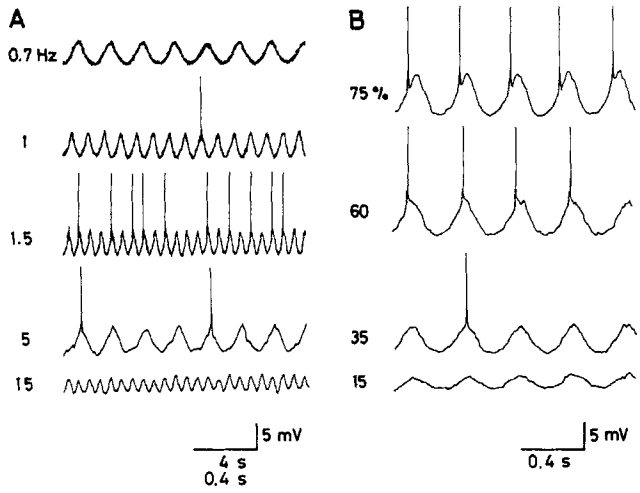

FIGURE 2. Typical responses of L-neurons to sinusoidal stimulus. (*A*) Responses of an L-neuron to a sinusoidal light stimulus with a modulation frequency of 0.5, 1.0, 1.5, 5, and 15 Hz. The depth of modulation was 60% and the mean illuminance was 0.2 $\mu W \cdot cm^{-2}$. (*B*) Responses to sinusoidal stimulus with a depth of modulation of 15, 35, 60, and 75%. The modulation frequency was 3 Hz and the mean illuminance was 0.2 $\mu W \cdot cm^{-2}$. A single spike is seen at the peak of the depolarizing phase of the voltage modulation. One cycle of light modulation induced only one spike, even when the depth of modulation was quite large (75%). *A* and *B* are from different L-neurons. The scales in *A* are 4 s for the 0.5-, 1-, and 1.5-Hz records and 0.4 s for the 5- and 15-Hz records.

Fig. 3 shows the peak-to-peak amplitude of the slow response of an L-neuron plotted against the modulation depth of the stimulus. To simplify the figure, only five series of responses to different modulation frequencies are shown. The stimulus had a mean illuminance of 2 $\mu W \cdot cm^{-2}$ (−1 log unit). The amplitude of the slow response depended almost linearly on the modulation depth of the stimulus, at least within the range of modulation depths of 80%. A similar linear relationship was observed over a wide range of frequencies (0.1–30 Hz), and also over a 3.6-log range of mean illuminance (0.005–20 $\mu W \cdot cm^{-2}$). The linear nature of the slow potential response facilitated analysis of the dynamic relationship between the slow potential and the spikes, using a sine wave–modulated light. If the slow potential response were

nonlinear and the response to sinusoidal stimulation had a serious nonlinear distortion, the light stimulation would be inadequate for a quantitative analysis of the relationship between the slow potential and the spikes.

General Characteristics of the Slow Spike Conversion Process

Fig. 4 *A* shows the relationship between the peak-to-peak amplitude of the slow potential response and the rate of spike generation at a modulation frequency of 1 Hz. The mean illuminance of the stimulus was −2 log units. There was a dead zone in which spikes were not generated. Beyond that zone, the spike rate increased with the increase in the amplitude of the slow response. The generation of the spike response is probabilistic, showing that the spike initiation has an internal noise. The plot is almost sigmoidal, with a linear part covering the spike rate ranging from 10 to 90%. Similar sinusoidal or quasilinear relationships between the amplitude of voltage

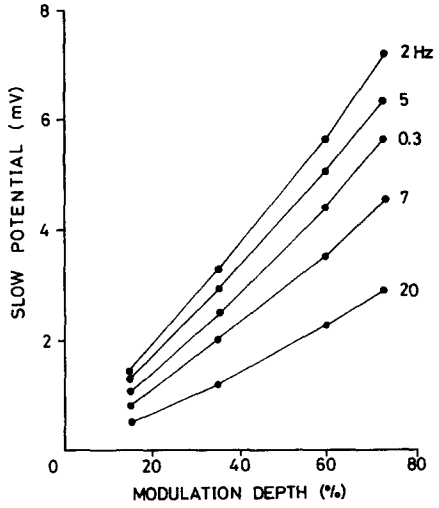

FIGURE 3. Peak-to-peak amplitude of the slow potential response of an L-neuron plotted against the modulation depth of the stimulus. The results obtained at five different modulation frequencies are shown. The amplitude of the slow potential response increased linearly with the depth of modulation of the stimulus. The mean illuminance of the stimulus was 2 $\mu W \cdot cm^{-2}$.

modulation and the spike rate were obtained over a frequency range of 0.1–20 Hz and over a mean illuminance range of 3.6 log units.

Fig. 4 *B* shows the relationship between the peak-to-peak amplitude of the slow potential response and the spike rate obtained at different frequencies. The results at a spike rate of between 10 and 90% are shown. The extrapolated straight lines are regression lines for each frequency. The lines cross the vertical axis at almost the same point. This suggests that the nonlinear threshold is frequency independent: the nonlinearity of the spike initiation process is static. On the other hand, the slope of the lines changes with the frequency, which indicates that the spike initiation process contains a dynamic linearity. In short, the spike initiation process contains a dynamic linearity and a static nonlinearity. A simple model for the spike initiation process will be proposed, based on these observations, in a later section (see Fig. 12).

Effects of Mean Illuminance on the Spike Threshold

Here we define 50% threshold as the peak-to-peak amplitude of the slow response at a spike rate of 50%. Further analysis was made using the 50% threshold. Fig. 5 *A*

shows the relationship between the 50% threshold and the modulation frequency, obtained at a mean illuminance range of 3.6 log units. In this experiment, a neuron was impaled, the ocellus was dark-adapted for 5 min, and the test began with −3.6-log ND filters interposed. After each sinusoidal test run (started after 60 s of adaptation), the density of the ND filter was decreased. After a test at the maximum illuminance (0 log), the sequence was reversed. This series was repeated four times. The 50% threshold was smallest at frequencies of ~0.5–5 Hz: the slow spike conversion process was bandpass. The 50% threshold at optimal frequencies, where the 50% threshold was smallest (~0.5–5 Hz), was unchanged over a mean illuminance range of 3.6 log units. However, the 50% threshold at frequencies of <0.5 Hz did change depending on the mean illuminance levels. The threshold was lower at a

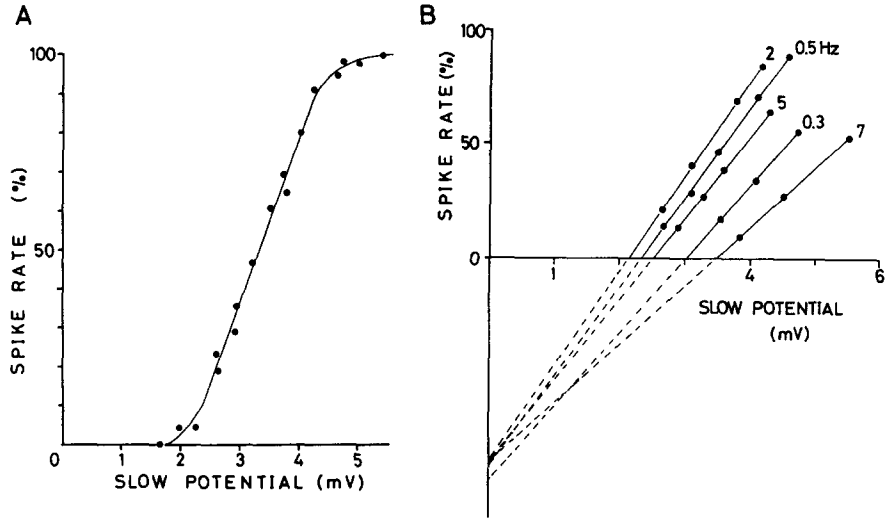

FIGURE 4. (*A*) The rate of spike generation plotted against the peak-to-peak amplitude of the slow potential response, obtained at a frequency of 1 Hz. The form of the curve was sigmoidal, with the linear part covering the range of spike rate of ~10–90%. (*B*) The spike rate plotted against the amplitude of slow response, obtained at five different frequencies. The extrapolated dashed lines are the regression lines for each frequency. These lines cross the vertical axis at almost the same point. The stimulus had a mean illuminance of 2 $\mu W \cdot cm^{-2}$.

dimmer mean illuminance. Similar observations of eight L-neurons were made repetitively, although the absolute value of the 50% threshold differed slightly (<30%) from preparation to preparation.

Fig. 5 *B* shows the phase characteristics of spike generation, measured from the peak of the potential modulation. Measurements were done from the records of responses in which the spike rate was ~50%. The phase of spike generation progressively led that of the slow potential with decreases in the frequency, which suggests that the process has a differential or change-sensitive nature. The variance of the phase was larger at a dimmer mean illuminance. The variance of the phase at −3.6 log units was about twice of that at 0 log units.

Fig. 6 shows actual recordings from an L-neuron exposed to low-frequency stimulation, at mean illuminances of −3.6 (upper trace) and of 0 (lower trace) log

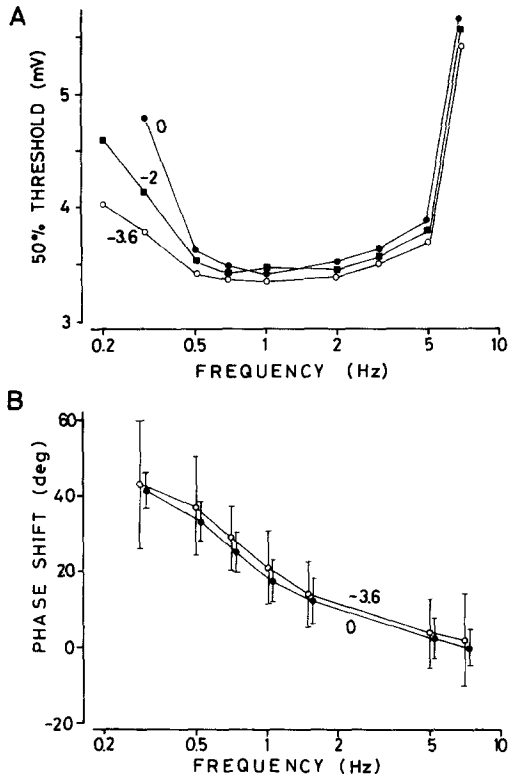

FIGURE 5. (*A*) 50% threshold of spike response, defined as the peak-to-peak amplitude of the potential modulation at a spike rate of 50%, plotted against the modulation frequency. The plots are from the responses of an L-neuron to sinusoidal lights with a mean illuminance of 0.005 (−3.6 log), 0.2 (−2 log), and 20 $\mu W \cdot cm^{-2}$ (0 log). (*B*) Phase characteristics of the spike response measured from the peak of the potential modulation. Measurements were made from the records of responses in which the spike rate was ~50% (40–60%), and the results at a mean illuminance of 0 log and −3.6 log are shown. The phase variance is larger at a dimmer illuminance (−3.6 log). *A* and *B* are from the same L-neuron.

units. The modulation depth of the stimulus was kept at 60% and the modulation frequency was kept at 0.2 Hz. Spikes could be seen in the −3.6-log record but not in the 0-log record, although the waveforms and the averaged peak-to-peak amplitudes of the modulation response were similar. This observation indicated that the 50% spike threshold is lower; i.e., a smaller amplitude of voltage modulation can produce spikes at a dimmer mean illuminance. In addition, more than one spike was frequently observed within one cycle of the potential modulation, when the mean illuminance was less than −3 log units and the frequency of modulation was below ~0.5 Hz. The increase in the spike number was accompanied by an increase in the variance of the phase of spike initiation.

Note that our analysis was designed for a system in which a single stimulus (single

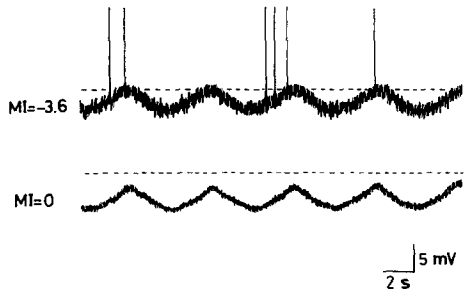

FIGURE 6. Responses of an L-neuron to sinusoidal lights with a mean illuminance of 0.005 (−3.6 log) or 20 $\mu W \cdot cm^{-2}$ (0 log). The stimuli had a modulation frequency of 0.2 Hz and a modulation depth of 60%. The dashed lines indicate the mean membrane potential in the dark (about −45 mV). Note that spikes are seen from the −3.6-log record but not from the 0-log record.

voltage modulation) produces a single effect (single spike), and had a limitation when multiple spikes occurred during a single modulation cycle. We defined the rate of spike generation as the number of modulation cycles in which spikes were generated, divided by the total number of cycles: the spike rate in this study does not reflect the number of spikes during a single modulation cycle. Thus, the 50% threshold, defined on the basis of the spike rate, is less informative about the actual spike response when multiple spikes occur during a cycle. However, our extended analysis (noise current stimulus combined with the sine wave light stimulus; see below) helped us understand which features of slow potential are relevant in the production of multiple spikes during a single modulation cycle.

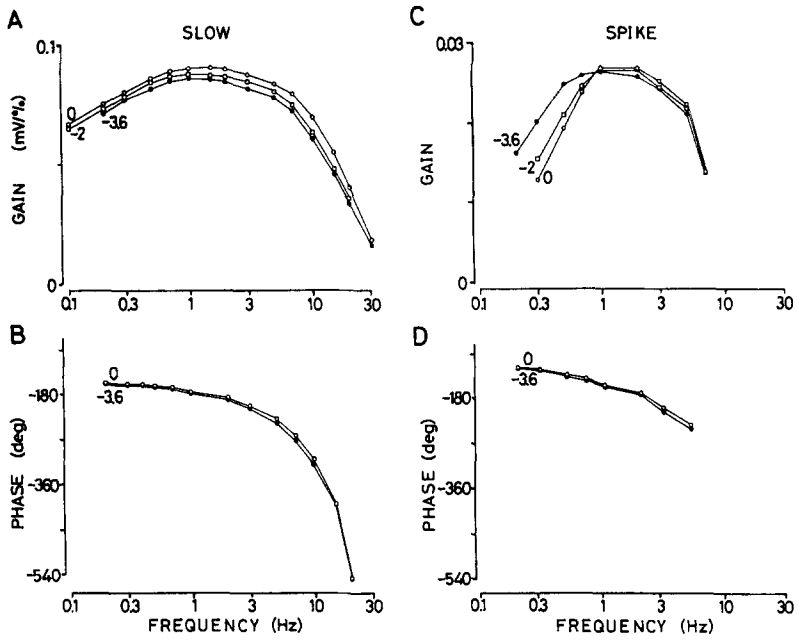

FIGURE 7. Gain and phase portion of the transfer characteristics from light to the slow potential response (*A* and *B*) and those from light to the spike response (*C* and *D*), obtained from an L-neuron over a mean illuminance range of 3.6 log units. The gain in *A* was defined as the slope of the response amplitude (millivolts) vs. the modulation depth of the stimulus (percentage) plot (see Fig. 3). The gain in *C* is the inverse of the modulation depth of the stimulus light (percentage) at a spike rate of 50%. The phase angles of the spike response (*D*) were measured from the peak illuminance of the light modulation.

Fig. 7 shows the gain and phase portion of the transfer characteristics from light to the slow potential response and of those from light to the spike response. The gain of the slow potential response was defined as the slope of the depth-response curve, i.e., the magnitude of the slow response (millivolts) divided by the depth of stimulus modulation (percentage). This definition is based on the observation that the slow potential response is almost linear (see Fig. 3). Because the depth represents the contrast between the stimulus and the adapting light, the gain is also the contrast sensitivity. The gain of the spike response was defined as the inverse of the depth of stimulus modulation (percentage) at a spike rate of 50%. We found for the gain

portion of the transfer characteristics (Fig. 7, *A* and *C*) that: (*a*) both the slow potential and spike responses had bandpass characteristics with optimal frequencies of ~0.5–5 Hz; (*b*) the spike response is more sharply bandpass than is the slow potential response; (*c*) the gain of the slow potential response is practically unchanged over a mean illuminance range of 3.6 log units: the gain is independent of the mean illuminance levels; (*d*) the gain of the spike response at optimal frequencies remains unchanged over a mean illuminance range of 3.6 log units; however, (*e*) at lower frequencies, the gain of the spike response changes depending on the mean level of illuminance. These differences reflect dynamic properties of the spike initiation process. The phase of the slow potential response is about −180 degrees at low frequency, which reflects that the sine of the response is negative-going (hyperpolarizing) and lags with increases in the stimulus frequency. A comparison of the phase of the slow potential and spike response shows that (*a*) the phase of the spike response leads that of slow potential response, and (*b*) the phases of both responses are affected little by the mean illuminance change, except that variance of the phase of the spike response changes depending on the mean illuminance, as shown in Fig. 5 *B*. We conclude that (*a*) the dynamics (frequency selectivity) of the slow potential response are independent of the mean illuminance levels, but (*b*) there is an enhancement of low-frequency sensitivity in the spike response at a dim mean illuminance: the dynamics of the spike response depend on the mean illuminance.

Effects of Noise and Mean Potential Level on the Spike Threshold

Fig. 6 also shows that (*a*) the magnitude of the spontaneous voltage fluctuation (voltage noise) is smaller under brighter illumination and (*b*) the mean potential level is more negative under brighter illumination (the dashed lines indicate the mean membrane potential in the dark). We considered that these may be the factors responsible for changes in the 50% spike threshold by changes in the mean illuminance.

The dependence of the mean potential level and the noise magnitude on the mean illuminance levels was examined. The L-neuron responded to steady illumination with a hyperpolarizing potential with a transient peak, and the potential reached a steady level within 30–40 s (Fig. 8 *A*). In the steady state, the membrane potential was more negative and the noise was less prominent under brighter illumination. Fig. 8 *B* shows the magnitude of the steady state hyperpolarization from the dark potential, plotted against the stimulus illuminance. Averages from five L-neurons are shown with the standard deviations. The membrane potential of L-neurons hyperpolarized ~0.8–1 mV for a 1-log increase in the stimulus illuminance, within a range from −4 to −1 log units. The membrane potential seemed to approach a constant level at the illuminance exceeding −1 log unit. Fig. 8 *C* shows the probability density functions (PDFs) of the noise obtained at a 4-log range of illuminance levels. The zero potential of the plot indicates the level of mean potential. The noise was reduced when the illuminance of the stimulus was increased. The noise reached a minimum at an illuminance of about −1 log unit, at which the half-width of the PDF was ~0.5 mV. Fig. 8 *D* shows power spectra of the noise obtained at a 4-log range of illuminance levels. The power spectra looked like a simple Lorenzian function, and most of the power was restricted to frequencies of less than ~50 Hz. This power was greatly reduced, with increases in the stimulus illuminance.

At least two possible sources for the noise were considered. First, the noise may reflect the electrical properties of the L-neuron: the noise may be due to a voltage-dependent noise source. In the dark or under dim illumination, the neuron may be more active than under brighter illumination because the membrane potential is more positive; thus, a larger voltage-related noise may be generated. Second, the noise may reflect that contained in the synaptic potential from photoreceptors. If the noise reflects electrical properties of the L-neuron, significant differences in the noise magnitude would be expected for an extrinsic current applied through the recording electrode. For example, when the dark-adapted L-neuron is hyperpolarized 3 mV by the extrinsic current, the noise would decrease

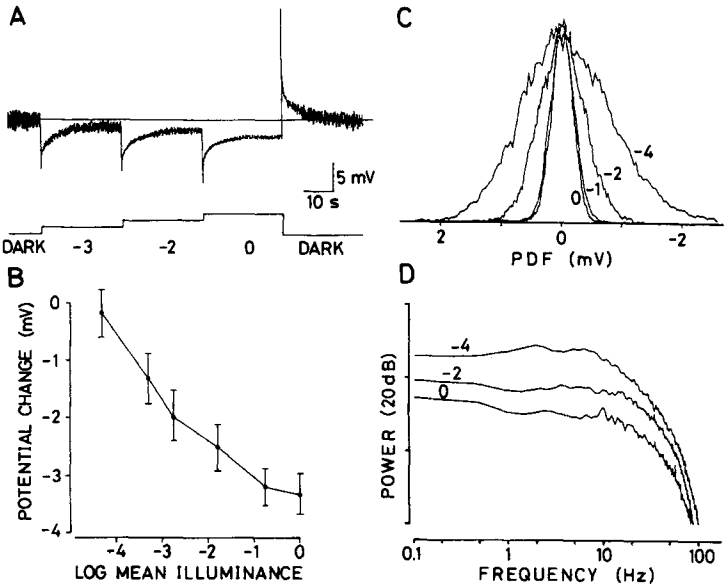

FIGURE 8. Steady state responses of an L-neuron to steady illumination. (*A*) Responses of an L-neuron to prolonged illumination. The light intensities are indicated as $\log_{10}$ attenuation (0 log units = 20 $\mu W \cdot cm^{-2}$). (*B*) Magnitude of steady state hyperpolarization from the dark potential plotted against the log of illuminance. Averages from five L-neurons are shown, with the standard deviations. (*C*) Probability density functions (PDFs) of the spontaneous voltage fluctuation (noise) during steady illumination of 0, −1, −2, and −4 log units. (*D*) Power spectra of the noise during steady illumination of 0, −2, and −4 log units.

to a value under a steady illumination of ~0 log units. Also, when the L-neuron is depolarized 3 mV under conditions of steady illumination of 0 log units, the noise would increase to a value seen in the dark. Before the current-injection experiments were done to test these possibilities, we measured the current-voltage relationship of L-neurons using double-barreled electrodes. Examples of recordings of the voltage responses to current stimuli are shown in Fig. 9 *B*, and a typical current-voltage relationship is shown in Fig. 9 *C*. The input resistance, the slope of the current-voltage plot, was ~1.6 MΩ in the dark and ~0.8 MΩ in the presence of a steady illumination of 0 log units. On the basis of these observations, we injected a negative current of 2 nA into a dark-adapted L-neuron to hyperpolarize it ~3 mV, or a posi-

tive current of 4 nA under illumination of 0 log units to depolarize the neuron ~3 mV (Fig. 9 *A*). In both cases, no prominent changes in the noise magnitude were observed. We thus conclude that the contributions of the voltage-dependent noise source to the noise seen in the L-neuron are small. The noise reflects that contained in synaptic potentials from photoreceptors.

In Fig. 10 *A*, steady or noise current was injected into an L-neuron during light stimulation, and the 50% threshold was measured. The mean illuminance of the

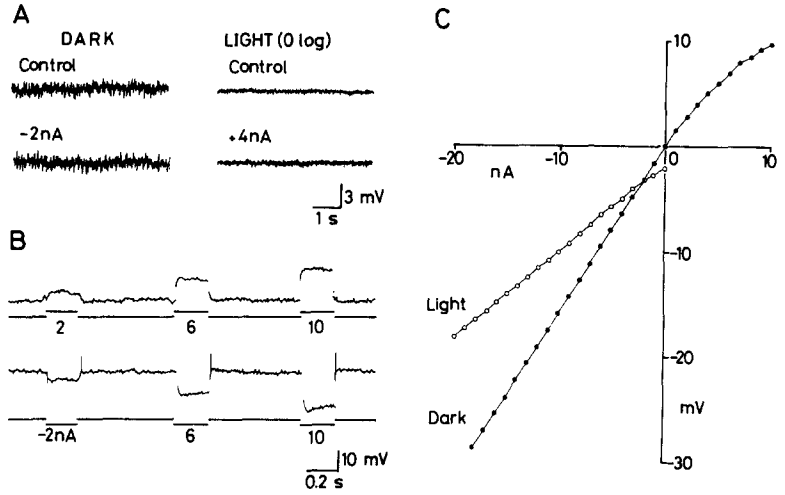

FIGURE 9. (*A*) Effects of steady current injection on the magnitude of noise. Neither a hyperpolarizing current of 2 nA applied in the dark nor a depolarizing current of 4 nA applied under steady illumination of 20 $\mu W \cdot cm^{-2}$ induced much change in the magnitude of noise. (*B* and *C*) Current-voltage relationship of an L-neuron measured using a double-barreled electrode. (*B*) Typical responses to depolarizing or hyperpolarizing current pulses recorded in the dark. The waveforms of the voltage response were almost step-like, while the strong current stimulus induced a response with a slight transient peak (see record for −10 nA). (*C*) Current-voltage plots of an L-neuron obtained in the dark (filled circles) and under steady illumination of 20 $\mu W \cdot cm^{-2}$ (open circles). Measurements were done at the peak of the voltage response. The dark potential (the zero potential of the plot) was about −45 mV. In the dark, the input resistance (the slope of the plot) was constant at ~1.6 MΩ between −30 and ~0 mV, and was smaller at a potential positive to the dark level. The input resistance was much smaller under illumination of 20 $\mu W \cdot cm^{-2}$. The averaged input resistance from five L-neurons was 1.6 ± 0.3 MΩ in the dark and 0.8 ± 0.2 MΩ under illumination of 20 $\mu W \cdot cm^{-2}$. The measured value of the input resistance of the dark-adapted L-neuron was similar to that measured from the locust L-neuron (1.7 MΩ on the average, Wilson, 1978*b*; 1.5 MΩ, Simmons, 1982).

stimulus was 0 log units, at which the mean membrane potential was ~3 mV negative to the dark level. There the noise was slight. A steady depolarizing current of 4 nA, estimated to depolarize the neuron ~3 mV based on the input resistance data (see Fig. 9 *C*), had no significant effect on the 50% threshold. We conclude that the chnage in the mean potential level is not the major cause of changes in the 50% threshold by changes in the mean illuminance. The noise current stimulation was made as follows. The potentials of an L-neuron were recorded under conditions of dim illumination (−3.6 log units) and then stored on analog tape. These stored

potentials were passed through an active low-cut filter to subtract the DC components and were used to drive a current-passing circuit. The output current of the circuit, which was applied to an L-neuron, had a waveform similar to that of the driving noise potential. The 50% threshold at low modulation frequencies became smaller when a noise current that had a peak-to-peak intensity of ~4 nA was injected (Fig. 10 *A*, open circles). The curve of the plot in the presence of noise current was similar to that observed under dim illumination (see Fig. 5 *A*). Similar results were repeatedly obtained with four L-neurons. In addition to the change in the 50% threshold, we observed that the noise current produced (*a*) an increase in the variance

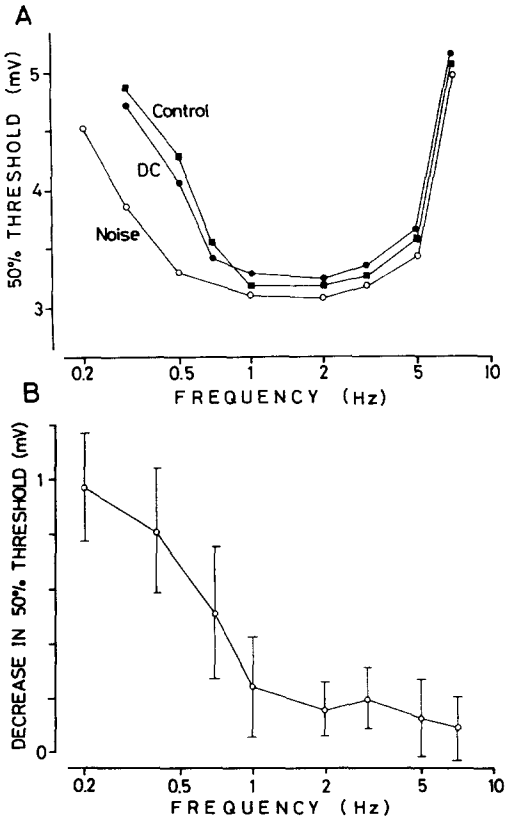

FIGURE 10. (*A*) Effects of noise current and steady current injection on the 50% threshold of an L-neuron. A noise current having a peak-to-peak amplitude of ~4 nA or a steady depolarizing current of 4 nA was injected during sinusoidal light stimulation. The light stimulus had a mean illuminance of 20 $\mu W \cdot cm^{-2}$. The estimated potential change produced by the injection of current of 4 nA was ~3 mV (the estimated input resistance at that mean illuminance was ~0.8 MΩ; see Fig. 9 *C*). The 50% threshold at a low-frequency range decreased when the noise current was injected. The steady depolarizing current had little effect on the 50% threshold. (*B*) The magnitude of the decrease in the 50% threshold induced by the noise current, plotted against the modulation frequency. An average from four L-neurons is shown. The procedure for the measurements was the same as that in *A*. The facilitatory effect of the noise on the spike initiation is more prominent at a lower frequency.

of the phase of spike generation and (*b*) an increase in the spike number for one modulation cycle when the frequency was low. These findings were similar to those observed with a dim mean illuminance. We concluded that the decrease in the spike threshold to a low-frequency potential modulation by the decrease in the mean illuminance was due to the increase in the noise variance: the noise had a facilitative effect on the initiation of the spike.

Fig. 10 *B* shows the frequency selectivity of the facilitative effect of the noise on the spike initiation. In the figure, the magnitude of the decrease in the 50% threshold, induced by a noise current, is plotted against the modulation frequency. The procedure for the measurements was the same as that of Fig. 10 *A*, and averaged data

from four L-neurons are shown. The facilitative effect of the noise on the spike initiation was more prominent at a lower modulation frequency and less prominent at a higher frequency. This can be explained as follows. When there is a subthreshold low-frequency potential modulation, the potential will remain just below the firing level for a longer period than at a higher frequency. Thus, the probability that the potential will reach the firing level by the superimposed noise will be higher. Similarly, the superimposed noise will produce repetitive firing if the potential remains near the firing level for a longer time than the refractory period of spike initiation.

Note that although the noise effect on the 50% spike threshold was highly frequency selective, the effect on the spike frequency might not be frequency selective, because of multiple times that a potential is near its peak at a high-frequency potential modulation. Our analysis was done not on the spike frequency but on the (50%) spike threshold, because L-neurons rarely produced trains of spikes and appeared to code signals in the form of solitary spikes (discrete events) rather than as the frequency of spike trains (analog signals).

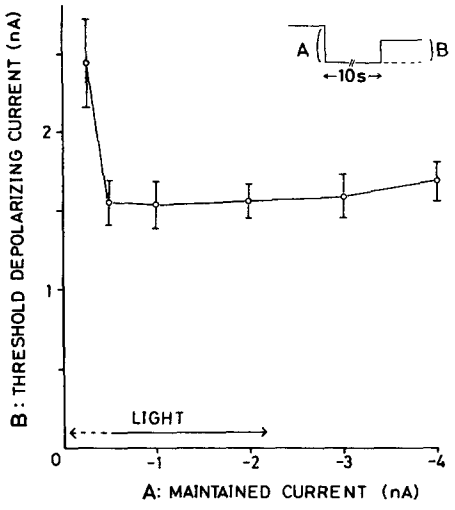

FIGURE 11. Magnitude of the threshold depolarizing current, the amount of depolarizing test-pulse required to trigger a spike (see inset *B*), plotted against the magnitude of maintained current, the amount of prepulse applied to maintain the potential at some fixed level (*A*). The membrane potential was first maintained at different levels for ~10 s, and then a test pulse was applied. Measurements were made in the dark. The dark potential was about −45 mV. The averages of six repetitive measurements from an L-neuron are shown with the standard deviations.

Steady State Inactivation of Spike Generation

It was an unexpected observation that the change in the mean membrane potential levels was not accompanied by a change in the 50% spike threshold. We did current-injection experiments to confirm this point. A hyperpolarizing prepulse was applied for ~10 s in a dark-adapted L-neuron to maintain the membrane potential at different levels; then a depolarizing test pulse was applied to trigger a spike. In Fig. 11, the threshold depolarizing current, which is the amount of current of the test pulse necessary to trigger a spike (see inset *B*), was plotted against the maintained current (*A*). We could expect that the relationship between threshold depolarization, the magnitude of step depolarization necessary to produce a spike, and maintained potential would be similar to the data in Fig. 11, because the input resistance was fairly constant in the range of current magnitude used (see Fig. 9 *C*). At a dark

potential, i.e., at a maintained current of 0 nA, depolarizing current pulses failed to evoke spikes: the neuron was completely inactivated at a dark potential (the same can be seen in Fig. 9 *B*). In the presence of a hyperpolarizing prepulse, the neuron generated a spike in response to a depolarizing current pulse. The membrane potential, under steady illumination of 0.005–20 $\mu W \cdot cm^2$, was ~0.8–3 mV negative to the dark potential (see Fig. 8 *B*). This potential range corresponds to the maintained current range between about -0.5 and -2 nA (marked as "light" in Fig. 11). In this range of maintained current, the threshold depolarizing current was fairly constant. This observation confirms that the change in the mean potential level had little effect on the spike threshold.

The observation in Fig. 11 suggests that there is a high degree of steady state inactivation in light-adapted L-neurons. The L-neuron was completely inactivated in the dark, and the membrane potential of the light-adapted L-neuron was <3.5 mV negative to that in the dark. Apparently the steady state inactivation produced a seemingly paradoxical relationship between the spike threshold and the mean potential levels; i.e., the spike threshold is independent of the mean potential levels.

DISCUSSION

Most studies on visual systems have been concerned with the response to steps of light given in the dark, and measurements have been made on the static aspects of the step-evoked responses. Therefore, little is known of the response dynamics to a light fluctuation around a mean illuminance. In particular, the dynamics of the cellular process that converts the slow potential into spikes are not well understood. In the vertebrate retina, dynamic properties of the spike response of ganglion cells have been studied (Schellart and Spekreijse, 1972; Victor and Shapley, 1979; Victor, 1987), but most of these studies concentrated on the dynamics of synaptic inputs into the cells, and less attention was directed to the dynamics of the spike initiation process.

Cockroach ocellar L-neurons do not discharge spontaneously, and a single cycle of voltage modulation produces either a single spike or very few spikes. The cockroach L-neurons probably encode signals in the form of a single spike or very few spikes; this is different from neurons in other visual systems, in which signals are, in most cases, encoded in the frequency of spike trains.

We examined the relationship between the slow potential and spikes of cockroach ocellar L-neurons, using a sinusoidally modulated light stimulus. We found that (*a*) the spike initiation process of the cockroach ocellar L-neuron is probabilistic (stochastic): the process has an internal noise; (*b*) the process has bandpass filtering properties; and (*c*) the process contains a dynamic linearity and a static nonlinearity. The observations suggest that a simple model, such as the integrate-and-fire model developed by Knight (1972*a*, *b*), may represent the actual spike initiation process. The final form of his model consists of a "forgetful integration" process, which is frequency dependent (dynamic) and linear, followed by a "stochastic firing" process, which is frequency independent (static) and nonlinear. Bryant and Segundo (1976) analyzed the spike initiation process of the *Aplysia* neuron and concluded that a similar model was quite accurate in predicting experimentally observed spike

discharges. Most recently, Sakuranaga et al. (1987) examined the spike discharge of catfish retinal ganglion cells and concluded that it can be modeled by an integrate-and-fire generator. These similarities among different preparations suggest that the integrate-and-fire model does represent the actual spike initiation process.

There is, however, some disagreement between our observations of the cockroach L-neuron and the integrator model. The forgetful-integrator model is nonadapting and always responds with tonic repetitive firing when stimulated with an adequate constant current. However, the cockroach L-neuron never generates tonic firing in response to a constant depolarizing current. This indicates that the spike initiation process of the L-neuron has a differential (or high-pass) property as well as an integrative (or low-pass) property. The model needs to include a bandpass filtering property in order to apply accurately to the actual spike initiation process of the cockroach L-neuron.

Knight (1972*a*, *b*) concluded that spike encoding in *Limulus* eccentric cells allows for a firing rate that is a replica of the shape of the stimulus. Sakuranaga et al. (1987) also concluded that signals contained in slow potentials remain substantially unchanged in the spike trains in catfish ganglion cells. In these neurons, little signal modification occurs during the spike initiation process. In the cockroach L-neuron, however, there are fundamental differences between the slow potential response and the spike response: (*a*) the slow potential response is linear, whereas the spike response is nonlinear; (*b*) the dynamics of the slow response are independent of the mean illuminance levels, whereas the dynamics of the spike response depend on the mean illuminance; and (*c*) the bandpass property of the spike response is sharper than that of the slow potential response. Therefore, we conclude that spike initiation in the L-neuron is an important step in visual signal processing. The function of the spike initiation process in the L-neuron is to filter out specific features from the slow potential signals (i.e., dimmings from the mean level), rather than to produce a replica of the slow potential.

There was a prominent enhancement of the low-frequency sensitivity in the spike response when the mean illuminance was low. A similar dependence of response dynamics (frequency dependence) on the levels of mean illuminance has been found in all the visual systems so far studied, including *Limulus* eyes (Fuortes and Hodgkin, 1964), insect compound eyes (Pinter, 1972; Dubs, 1981), and vertebrate retina (Naka et al., 1979, 1987; Tranchina et al., 1983; Chappell et al., 1985). In these visual systems, such a dependence is prominent at any level of the system, including photoreceptor cells, whereas in the cockroach ocellar system, the slow potential response of L-neuron exhibits no such dependence. It is a notable finding that in the cockroach ocellus, a coupling between the response dynamics and the mean illuminance levels is produced at the spike initiation process of L-neurons, not in the receptor cells.

The spike response of the L-neuron had a bandpass filtering property with an optimal frequency range of ~0.5–5 Hz, which reflects that both the slow potential response and the spike initiation (slow spike conversion) process had optimal frequency ranges of ~0.5–5 Hz. This optimal frequency range is much lower than that noted in vertebrate retinal ganglion cells (Victor and Shapley, 1979; Sakuranaga et al., 1987). The difference may reflect the fact that cockroach L-neurons are

designed to detect a change in the illumination averaged over a wide receptive field (note that the 10,000 ocellar photoreceptors converge onto only four L-neurons), whereas vertebrate retinal ganglion cells are designed to detect a small target within a narrow receptive field.

The bandpass property of the spike initiation process apparently reflects the activation and inactivation kinetics of the voltage-dependent current of the L-neuron. If the rate of voltage change is slow with respect to the inactivation time constant of the inward current, the conductance change for the inward current would be low and no action potential would be generated. As the frequencies of voltage modulation are increased, action potentials will be generated. However, at high frequencies, when the rate of change of voltage is rapid with respect to the time constant of activation of the inward current, there would not be sufficient time to activate the inward current and thus no action potentials would be generated. In short, an inactivation time constant limits the low-frequency response and an activation time constant limits the high-frequency response. Another factor that limits the low-frequency response is the activation time constant of the outward current, because the effects of activation of the outward current are the same as for the inactivation of the inward current. The optimal frequencies of the spike initiation process of the cockroach ocellar L-neuron (0.5–5 Hz) are much lower than those of the squid giant axon (50–80 Hz; Guttman et al., 1980). This difference indicates that the activation time constant of the inward current of the cockroach L-neuron (probably a calcium current; Mizunami et al., 1987) is slow in comparison with that of the inward sodium current in squid giant axon.

The noise in the second-order visual neurons has been noted in barnacle ocelli (Stuart and Oertel, 1978), *Limulus* eyes (Dodge et al., 1968), insect ocelli (Wilson, 1978*b*), insect compound eyes (Laughlin, 1973), and vertebrate retina (Ashmore and Copenhagen, 1983). In the present study, we found that the noise facilitates spike initiation; that is, it lowers the spike threshold. Noise has usually been discussed in relation to the signal-to-noise ratio, in which the noise was thought to disturb signal detection. Our finding suggests that, on the contrary, the noise has a positive role in signal detection.

The noise in the L-neuron was derived from synaptic inputs from the photoreceptors. The underlying mechanism remains to be determined. Possible sources of the noise are: (*a*) random photon capture of the photoreceptor cells, which results in a discrete bump response (photon noise), (*b*) random isomerization of the rhodopsin (transducer noise), and (*c*) random release of the transmitter substances from photoreceptors (synaptic noise). The first is attributed to properties of light input (extrinsic noise) and the latter two are intrinsic noise.

In the dark, the L-neuron was completely inactivated and no spikes were induced by extrinsic depolarizing current. Apparently there was a high degree of steady state inactivation in the light-adapted L-neuron, because the hyperpolarization resulting from the steady illumination was relatively small (<3.5 mV).

The change in the mean potential levels was not accompanied by a change in the spike threshold, which reflects the presence of a steady state inactivation. Functionally, this keeps the spike threshold unchanged over a wide range of mean illuminance. A similar relationship between maintained potential and threshold depolarization has

been noted in squid giant axon in the presence of a large depolarizing DC bias, in which there might be a steady state inactivation of the inward current (Holden, 1976).

The final goal of our analysis was to answer the question of which features of the slow potential are relevant in spike initiation. We were successful in answering this question in a quantitative manner. However, the complete answer to this question needs a prediction of the actual spike response when the history of slow potential response is known. For a further prediction of the actual spike response, we need to develop a model for the spike initiation process.

In conclusion, we propose a simple model for signal processing in the cockroach ocellus (Fig. 12). Light signals that enter the ocellus are passed through a bandpass linear filter and produce a slow potential response in L-neurons. The linear filter consists of photoreceptors and synapses between photoreceptors and L-neurons. The details of its filtering properties have been discussed (Mizunami et al., 1986). The slow potential contains noise. The noise, whose exact origin remains to be determined, reflects that contained in the synaptic potential from photoreceptors.

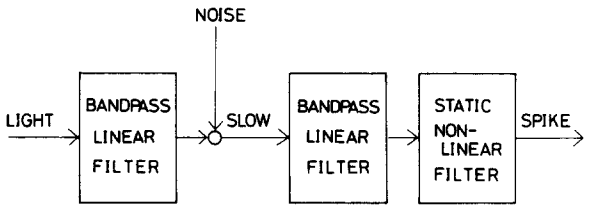

FIGURE 12. A model for signal processing in cockroach ocellus. Light signals are passed through a bandpass linear filter and produce a slow potential response in L-neurons. The slow potential contains a noise, which reflects that contained in the synaptic potential from photoreceptors. The slow potential is further passed through a linear/nonlinear cascade and produces a spike discharge. The linear filter is bandpass, and the nonlinear filter is a static threshold. For details, see text.

The slow potential is passed through a linear/nonlinear cascade and produces a spike discharge. The linear filter is bandpass, having both a differential and an integrative nature. The nonlinear filter is a static threshold with a sigmoidal (probabilistic) input/output relationship. Although the effectiveness of the model in predicting the actual responses of cockroach ocellar neurons remains to be determined, the model will be a good base for further understanding signal processing in the cockroach ocellar system.

Ocellar L-neurons make output synapses onto several types of third-order neurons in the ocellar tract (Toh and Hara, 1984; Mizunami and Tateda, 1986). An important question that remains unanswered is whether the slow potential signals or the spike signals of L-neurons or both are encoded in the third-order neurons. Fig. 13 shows typical responses of two types of third-order neurons, called OL-I neurons (type I neurons projecting into the optic lobe) and D-I neurons (type I neurons descending to the thoracic ganglia; Mizunami and Tateda, 1986), to sinusoidal light stimulation. One type of third-order neuron, the OL-I neuron, had a spontaneous spike discharge and exhibited a modulation of the spike frequency around a mean (Fig. 13 *A*). The pattern of the response was similar to, although not the same as, that of the slow potential response of the L-neurons. The other type, the D-I neuron, had no

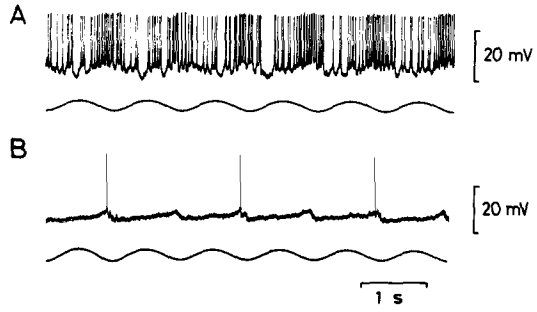

FIGURE 13. Typical responses of two types of third-order neurons to sinusoidal light stimulation. One type of third-order neuron, the OL-I neuron (type I neuron projecting into the optic lobe), showed sinusoidal modulation of spike frequency (*A*), whereas the other type, the D-I neuron (type I neuron descending to the thoracic ganglia), generated solitary spikes at the decremental phase of light modulation (*B*). The anatomy of these neurons and their responses to step light given in the dark can be seen elsewhere (Mizunami and Tateda, 1986). The lower traces indicate the stimulus light, monitored by a photodiode. The stimulus had a modulation frequency of 1 Hz and a modulation depth of 50%. The mean illuminance was 2 $\mu W \cdot cm^{-2}$.

spontaneous spike activity and exhibited single spikes at the decremental phase of light modulation (Fig. 13 *B*). The pattern of the response was similar to that of the spike response of L-neurons. The observations suggest that both slow potential signals and spike signals in L-neurons are encoded into the third-order neurons. We conclude that the role of ocellar L-neurons is to produce two kinds of signals, linear (slow potential) and nonlinear (spike). The details of signal processing in third-order neurons will be dealt with in a future study.

We thank Professor Ken-Ichi Naka, The National Institute for Basic Biology, for the use of equipment, and M. Ohara, Kyushu University, for helpful comments on the manuscript.

This study was supported in part by grants from the Ministry of Education of Japan.

Original version received 10 June 1987 and accepted version received 5 January 1988.

REFERENCES

Ashmore, J. F., and D. R. Copenhagen. 1983. An analysis of transmission from cones to hyperpolarizing bipolar cells in the retina of the turtle. *Journal of Physiology.* 340:569–597.

Bryant, H. L., and J. P. Segundo. 1976. Spike initiation by transmembrane current: a white-noise analysis. *Journal of Physiology.* 260:279–314.

Chappell, R. L., and J. E. Dowling. 1972. Neural organization of the median ocellus of the dragonfly. I. Intracellular electrical activity. *Journal of General Physiology.* 60:121–147.

Chappell, R. L., K.-I. Naka, and M. Sakuranaga. 1985. Dynamics of turtle horizontal cell response. *Journal of General Physiology.* 86:423–453.

Dodge, F. A., B. W. Knight, and J. Toyoda. 1968. Voltage noise in *Limulus* visual cells. *Science.* 160:88–90.

Dowling, J. E., and R. L. Chappell. 1972. Neural organization of the median ocellus of the dragonfly. II. Synaptic structure. *Journal of General Physiology.* 60:148–165.

Dubs, A. 1981. Non-linearity and light adaptation in the fly photoreceptors. *Journal of Comparative Physiology.* 144:53–59.

Fuortes, M. G. F., and A. L. Hodgkin. 1964. Changes in time scale and sensitivity in the ommatidia of *Limulus*. *Journal of Physiology.* 172:239–263.

Goodman, L. J. 1981. Organization and physiology of the insect dorsal ocellar system. *In* Handbook of Sensory Physiology. Vol. VII/6C. Springer-Verlag, Berlin. 201–286.

Guttman, R., L. Feldman, and E. Jakobsson. 1980. Frequency entrainment of squid axon membrane. *Journal of Membrane Biology.* 56:9–18.

Holden, A. V. 1976. The response of excitable membrane models to a cyclic input. *Biological Cybernetics.* 21:1–7.

Knight, B. W. 1972*a*. Dynamics of encoding in a population of neurons. *Journal of General Physiology.* 59:734–766.

Knight, B. W. 1972*b*. The relationship between the firing rate of a single neuron and the level of activity in a population of neurons. Experimental evidence for resonant enhancement in the population response. *Journal of General Physiology.* 59:767–778.

Knight, B. W., J.-I. Toyoda, and F. A. Dodge. 1970. A quantitative description of the dynamics of excitation and inhibition in the eye of *Limulus*. *Journal of General Physiology.* 56:421–437.

Laughlin, S. B. 1973. Neural integration in the first optic neuropile of dragonflies. I. Signal amplification in dark-adapted second order neurons. *Journal of Comparative Physiology.* 84:335–355.

Mizunami, M., and H. Tateda. 1986. Classification of ocellar interneurones in the cockroach brain. *Journal of Experimental Biology.* 125:57–70.

Mizunami, M., H. Tateda, and K.-I. Naka. 1986. Dynamics of cockroach ocellar neurons. *Journal of General Physiology.* 88:275–292.

Mizunami, M., S. Yamashita, and H. Tateda. 1982. Intracellular stainings of the large ocellar second order neurons in the cockroach. *Journal of Comparative Physiology.* 149:215–219.

Mizunami, M., S. Yamashita, and H. Tateda. 1987. Calcium-dependent action potentials in the second-order neurones of cockroach ocelli. *Journal of Experimental Biology.* 130:259–274.

Naka, K.-I., R. Y. Chan, and S. Yasui. 1979. Adaptation in catfish retina. *Journal of Neurophysiology.* 42:441–454.

Naka, K.-I., M.-A. Itoh, and R. L. Chappell. 1987. Dynamics of turtle cones. *Journal of General Physiology.* 89:321–337.

Pinter, R. B. 1972. Frequency and time domain properties of retinular cells of the desert locust (*Schistocerca gregalia*) and the house cricket (*Acheta domesticus*). *Journal of Comparative Physiology.* 77:383–397.

Ruck, P. 1961. Electrophysiology of the insect dorsal ocellus. I. Origin of components of the electroretinogram. *Journal of General Physiology.* 44:605–627.

Sakuranaga, M., Y.-I. Ando, and K.-I. Naka. 1987. Dynamics of ganglion cell response in the catfish and frog retina. *Journal of General Physiology.* 90:229–259.

Schellart, N. A. M., and H. Spekreijse. 1972. Dynamic characteristics of retinal ganglion cell response in goldfish. *Journal of General Physiology.* 59:1–21.

Simmons, P. J. 1982. Transmission mediated with and without spikes at connexions between large second-order neurons of locust ocelli. *Journal of Comparative Physiology.* 147:401–414.

Stuart, A. E., and D. Oertel. 1978. Neural properties underlying processing of visual information in the barnacle. *Nature.* 275:287–290.

Toh, Y., and S. Hara. 1984. Dorsal ocellar system of the American cockroach. II. Structure of the ocellar tract. *Journal of Ultrastructure Research.* 86:133–148.

Toh, Y., and H. Sagara. 1984. Dorsal ocellar system of the American cockroach. I. Structure of the ocellus and ocellar nerve. *Journal of Ultrastructure Research.* 86:119–134.

Tranchina, D., J. Gordon, and R. Shapley. 1983. Spatial and temporal properties of luminosity horizontal cells in the turtle retina. *Journal of General Physiology.* 82:573–598.

Victor, J. D. 1987. The dynamics of the cat retinal X cell centre. *Journal of Physiology.* 386:219–246.

Victor, J. D., and R. M. Shapley. 1979. Receptive field mechanisms of cat X and Y retinal ganglion cells. *Journal of General Physiology.* 74:275–298.

Weber, G., and M. Renner. 1976. The ocellus of the cockroach, *Periplaneta americana* (Blattariae). Receptory area. *Cell and Tissue Research.* 168:209–222.

Wilson, M. 1978*a*. Generation of graded potential signals in the second order cells of locust ocellus. *Journal of Comparative Physiology.* 124:317–331.

Wilson, M. 1978*b*. The origin and properties of discrete hyperpolarizing potentials in the second order cells of locust ocellus. *Journal of Comparative Physiology.* 128:347–358.

Yamasaki, T., and T. Narahashi. 1959. The effects of potassium and sodium ions on the resting and action potentials of the cockroach giant axon. *Journal of Insect Physiology.* 3:146–158.